



Synthesis of porphyrin indolin-2-one conjugates via palladium-catalyzed amination reactions

José C.J.M.D.S. Menezes^a, Ana M.V.M. Pereira^a, Maria G.P.M.S. Neves^a, Artur M.S. Silva^a, Sérgio M. Santos^b, Sabrina T. Martinez^c, Bárbara V. Silva^c, Ângelo C. Pinto^c, José A.S. Cavaleiro^{a,*}

^a Department of Chemistry and QOPNA, University of Aveiro, 3810-193 Aveiro, Portugal

^b Department of Chemistry and CICECO, University of Aveiro, 3810-193 Aveiro, Portugal

^c Instituto de Química-CT, Bloco A, Universidade Federal do Rio de Janeiro, Cidade Universitária, 21941-970 Rio de Janeiro, RJ, Brazil

ARTICLE INFO

Article history:

Received 16 March 2012

Received in revised form 4 July 2012

Accepted 9 July 2012

Available online 15 July 2012

Keywords:

Porphyrin

Indolin-2-one

Palladium

Phosphine ligand

C–N coupling

Buchwald–Hartwig

Halogen position

Heating condition

B3LYP

ABSTRACT

New porphyrin indolin-2-one conjugates were synthesized via palladium-catalyzed amination reactions of iodinated and dibrominated indolin-2-one derivatives with (2-amino-5,10,15,20-tetraphenylporphyrinato)nickel(II). The combination of palladium catalysts and the phosphine ligand dicyclohexylphosphino-2',4',6'-triisopropylbiphenyl (XPhos) is an effective methodology for catalyzing the coupling of 5-iodo-, 5,7-dibromo- and 4,6-dibromo-1,3,3-trimethylindolin-2-one with 2-aminoporphyrin to give the corresponding mono-(2-aminoporphyrinyl)- and di-(2-aminoporphyrinyl)-substituted indolin-2-ones in satisfactory yields under mild conditions. The mono brominated porphyrinic derivatives also underwent cross-coupling reactions under similar catalytic conditions. The studies also demonstrated that the course of the coupling process depends on factors, such as the catalytic system, number and position of the halogen substituents and the heating condition. Insights into the reactivity trends of the 5-iodo; 4,6- and 5,7-dibrominated indolin-2-one derivatives was carried out using theoretical calculations performed using density-functional theory with the B3LYP functional.

© 2012 Elsevier Ltd. All rights reserved.

1. Introduction

The chemical and physical properties displayed by porphyrins render them appealing compounds for several applications. Supramolecular chemistry, biomimetic models for photosynthesis, catalysis, and medicinal applications, namely as photosensitizers in the photodynamic therapy (PDT) of tumours, are some of these significant examples.¹ As a result, several research groups have focused on the synthesis and chemical transformation of porphyrins into derivatives with new and well-defined substitution patterns that may turn them into possible candidates for several applications. Among the available synthetic tools for porphyrin functionalization,² the modification of a porphyrin macrocycle using the Buchwald–Hartwig palladium-catalyzed amination has emerged as a powerful approach for the formation of carbon–nitrogen bonds.³

The indolin-2-one, or oxindole moiety, is the basic nucleus of several natural and synthetic products with wide biological

activity.⁴ Indolin-2-ones are endogenous compounds found in mammalian body fluids and tissues, ubiquitously distributed in the central nervous system (for example, isatin is found in brain cells and other tissues in humans), that have shown an extensive range of biological effects, including antibacterial, antifungal, anticonvulsant, antiviral, anticancer and antiproliferative activities.⁵

The copper(II) complexes of indolin-2-one derived ligands **1** (Fig. 1) were also reviewed as potential antitumoral agents, based on the proposal of a synergic effect with the already demonstrated capability of such ligands to influence the angiogenesis and apoptosis processes.⁶

Sunitinib (Sutent[®]) **2** is an oral indolin-2-one multitargeted kinase inhibitor that is employed in the treatment of gastrointestinal stromal tumours (GISTs), renal cell carcinomas (RCCs) and pancreatic net. Because of its effectiveness, the activity of this drug is currently being evaluated in non-small cell lung, prostate, breast cancer and others.⁷

The molecule MI-219 **3** blocks the MDM2–p53 interaction and reactivates the p53 gene. This compound is undergoing preclinical development and is already being considered in clinical trials.⁸ Recently, a series of sixteen ferrocenyl indolin-2-ones with *E* or *Z* configurations, compounds of types **4** and **5**, have been synthesized

* Corresponding author. Tel.: +351 234 370 717; fax: +351 234 370 084; e-mail address: jcavaleiro@ua.pt (J.A.S. Cavaleiro).

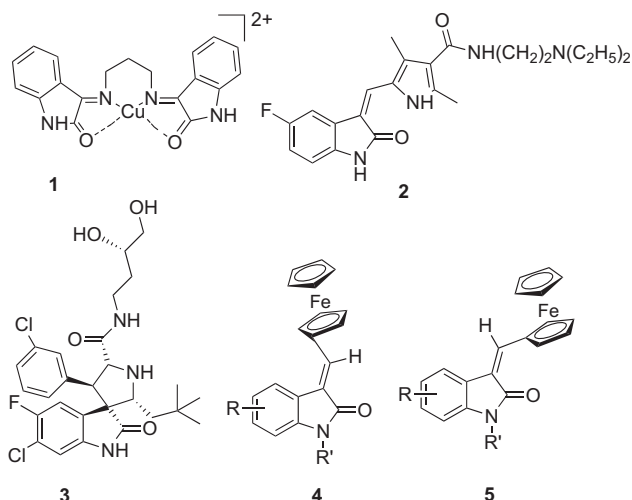


Fig. 1. Structures of indolin-2-one analogues 1–5 with biological activity.

and evaluated for inhibiting migration of breast tumour cells; promising results have been put forward.⁹ The biological effect of ferrocenyl indolin-2-ones has also been studied by Spencer et al.,¹⁰ those compounds have demonstrated to be potent inhibitors of the protein vascular endothelial growth factor (VEGFR) and platelet-derived growth factor receptor (PDGFR) kinases.

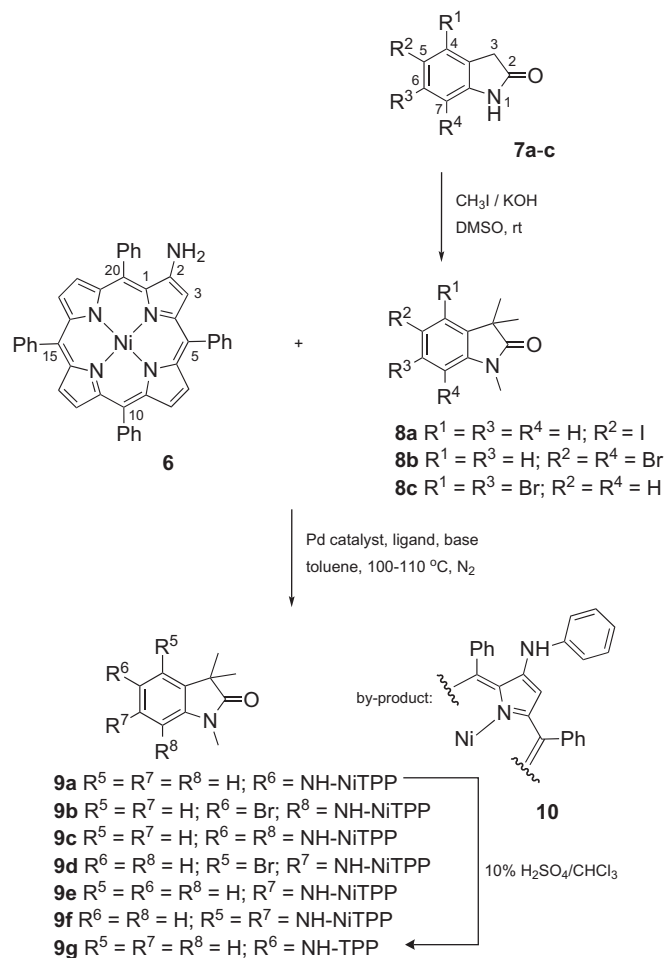
In this context, the synthesis of molecules with dual functions is considered a good strategy for the discovery of new drugs. Those molecules can be achieved by coupling entities containing well-established pharmacological activities. Therefore, a work target has been the study of the formation of carbon–nitrogen bonds between porphyrins and indolin-2-ones to obtain novel molecular frameworks with possible applications in medicinal therapeutics.

2. Results and discussion

The synthetic strategy to prepare the new porphyrin indolin-2-one conjugates **9a–g** was based on Buchwald–Hartwig palladium-catalyzed amination reactions involving the iodinated and dibrominated indolin-2-one derivatives **8a–c** and (2-amino-5,10,15,20-tetraphenylporphyrinato)nickel(II) **6**¹¹ [Ni(II)–2-NH₂–TPP] (Scheme 1).

The presence of amide functions and halide substituents in the starting indolin-2-one molecules **7a–c**¹² can give rise to self coupled products under the Buchwald–Hartwig palladium-catalyzed amination reactions. Therefore it is necessary to carry out a derivatization of such reagents. In fact, in the presence of Pd(OAc)₂ and *rac*-BINAP or XPhos (Fig. 2), and KO^tBu as base, no coupling product of **7a** with porphyrin **6** was obtained, the porphyrin **6** being totally recovered. In such way the trimethyl derivatives **8a–c** were obtained by methylation of indolin-2-ones **7a–c** with methyl iodide in DMSO in the presence of KOH¹³ (Scheme 1); the obtained compounds were characterized by ¹H NMR (with the signals corresponding to the proton resonances of the *gem*-dimethyl and *N*-methyl groups in the region of ~1.5 and ~3.5 ppm, respectively) and HRMS analysis.

Using the *rac*-BINAP catalytic system and similar reaction conditions, we performed the coupling of Ni(II)–2-NH₂–TPP **6** with 5-iodo-1,3,3-trimethylindolin-2-one¹⁴ **8a** (2 equiv) (Table 1, entry 1). The reaction was ended 24 h later, and after workup, two major compounds were isolated by preparative TLC. The HRMS spectrum of the porphyrinic derivative with lower *R_f* showed a peak at *m/z* 858.2611 corresponding to the M⁺ ion¹⁵ of the expected 5-(2-aminoporphyrinyl)-indolin-2-one **9a** (15% yield) (vide infra). The by-product, obtained in 29% yield, showed a peak at *m/z* 761.2 in its



Scheme 1. Synthesis of porphyrin indolin-2-one conjugates **9a–g**.

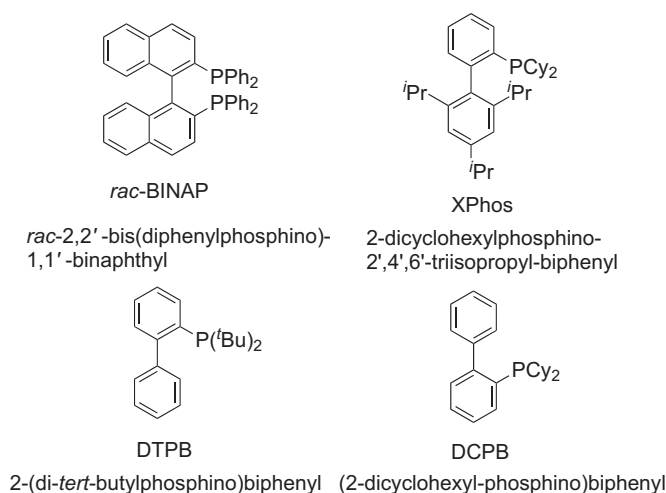


Fig. 2. Structures of the used phosphine ligands.

MS spectrum and the ¹H NMR spectrum indicated that a phenyl group has been attached to the porphyrin core. The structure of (2-phenylamino-5,10,15,20-tetraphenylporphyrinato)nickel(II) (**10**, Scheme 1) was confirmed by comparison with an authentic sample.^{3f} The possible formation of this compound can be justified through the transfer of a phenyl group from the phosphine ligand, *rac*-BINAP, to the metal centre followed by an eliminative reduction

Table 1
Catalyst, ligand, base and heating condition effects on palladium-catalyzed amination reaction of 5-iodo-1,3,3-trimethylindolin-2-one **8a** with Ni(II)–2-NH₂–TPP **6**^a

Entry	Catalyst; ligand	Base	Heating	9a Yield %	10 Yield %	Recovered 6 %
1	Pd(OAc) ₂ ; <i>rac</i> -BINAP	KO ^t Bu	Classical	15	29	—
2	Pd(OAc) ₂ ; XPhos	KO ^t Bu	Classical	35 ^b /53 ^c	—	34
3	Pd(OAc) ₂ ; XPhos	Cs ₂ CO ₃	Classical	19 ^b /23 ^c	—	16
4	Pd(OAc) ₂ ; XPhos	KO ^t Bu	MW	32 ^b /64 ^c	—	50
5 ^d	Pd(OAc) ₂ ; XPhos	KO ^t Bu	Classical	38 ^b	—	75
6	Pd(OAc) ₂ ; DTPB	KO ^t Bu	Classical	22 ^b /26 ^c	—	16
7	Pd(OAc) ₂ ; DTPB	KO ^t Bu	MW	5 ^b /9 ^c	—	42
8	Pd(OAc) ₂ ; DCPB	KO ^t Bu	Classical	13 ^b /18 ^c	—	28
9	(PPh ₃) ₄ Pd; XPhos	KO ^t Bu	Classical	81	—	—

^a The reactions were carried out at 100–110 °C in dry toluene for 24 h (classical heating) or 30 min (microwave irradiation), under N₂, with 1 equiv of Ni(II)–2-NH₂–TPP **6**, 2 equiv of indolin-2-one **8a**, 0.29 equiv of Pd catalyst and 0.26 equiv of ligand in the presence of 2.1 equiv of base.

^b Direct yield.

^c Yield based on recovered Ni(II)–2-NH₂–TPP **6**.

^d The reaction was performed using 5 equiv of Ni(II)–2-NH₂–TPP **6** and 1 equiv of indolin-2-one **8a**.

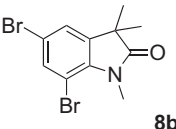
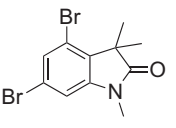
step in the catalytic cycle. The mechanisms involving this undesirable P–C bond cleavage of transition metal–phosphine complexes have been reviewed.¹⁶

To circumvent this exchange reaction, we selected the biphenyl ligand XPhos, (Fig. 2), to perform the coupling between **6** and **8a** in presence of different bases (Table 1, entries 2 and 3). A better yield of the desired product **9a** was obtained in the presence of KO^tBu when compared with the one obtained with Cs₂CO₃ (35% vs 19%). Additional experiments under microwave irradiation¹⁷ revealed that similar yields can be achieved in shorter reaction times (30 min vs 24 h) accompanied by a reduction of porphyrin **6** decomposition (Table 1, entry 4). A slight improvement in the yield of **9a** was observed by changing the ratio of porphyrin/indolin-2-one for 5:1 (Table 1, entry 5). No substantial improvement in the yield was observed when the used ligand was DTPB, (Fig. 2), under classical or MW heating conditions (Table 1, entries 6 and 7). The other phosphine ligand also tested, the DCPB, (Fig. 2), gave a low

as catalyst, ethylene glycol as ligand, K₃PO₄ as base and 1,4-dioxane as solvent, did not lead to the formation of the expected 5-(2-aminoporphyrinyl)-indolin-2-one **9a**, and the unreacted porphyrin **6** was recovered.

Based on the results obtained for product **9a**, similar studies with 5,7- and 4,6-dibromo-indolin-2-ones **8b** and **8c** were performed. When the palladium-catalyzed amination reaction of 5,7-dibromo-1,3,3-trimethylindolin-2-one **8b** with Ni(II)–2-NH₂–TPP **6** was carried out using a ratio 1:2 of porphyrin/indolin-2-one in presence of XPhos and KO^tBu (Table 2, entry 1), two products were isolated. The detailed 2D NMR and mass spectrometry analysis indicated that the compound with higher R_f is the mono-coupled product 7-(2-aminoporphyrinyl)-5-bromo-indolin-2-one **9b** (26% yield) while the other one is the bis-coupled product **9c** (9% yield). Interestingly, even by using an excess of indolin-2-one **8b**, which should result in the linkage of the porphyrin moiety at the 5' or 7'-position of **8b**, we isolated the compound **9c** bearing two porphyrin units.

Table 2
Compounds **6/8b,c** ratio, catalyst, ligand and heating condition effects on palladium-catalyzed amination reaction of indolin-2-one **8b,c** with Ni(II)–2-NH₂–TPP **6**^a

Entry	Catalyst; ligand	6/8b Ratio	Heating	9b Yield %	9c Yield %	9a Yield %	Recovered 6 %	
 8b	1	Pd(OAc) ₂ ; XPhos	1:2	Classical	26	9	—	13
	2	Pd(OAc) ₂ ; XPhos	1:2	MW	41	8	—	41
	3	Pd(OAc) ₂ ; XPhos	1.5:1	Classical	28	13	—	45
	4	Pd(OAc) ₂ ; XPhos	1.5:1	MW	38	14	—	28
	5	Pd(OAc) ₂ ; XPhos	3:1	Classical ^b	14	5	—	72
	6	Pd(OAc) ₂ ; DTPB	1.5:1	Classical ^c	—	11	18	31
	7	Pd(OAc) ₂ ; DTPB	2:1	Classical ^c	—	14	35	18
	8	(PPh ₃) ₄ Pd; XPhos	2:1	Classical ^c	—	18	53	31
Entry	Catalyst; ligand	6/8c Ratio	Heating	9d Yield %	9e Yield %	9f Yield %	Recovered 6 %	
 8c	9	Pd(OAc) ₂ ; XPhos	1:2	Classical	44	15	—	13
	10	Pd(OAc) ₂ ; XPhos	1:2	MW	63	14	—	2
	11	Pd(OAc) ₂ ; DTPB	1:2	Classical	64	—	—	—
	12	Pd(OAc) ₂ ; DTPB	2:1	Classical	33	—	7	27
	13	(PPh ₃) ₄ Pd; XPhos	1:2	Classical	23	22	—	—
	14	(PPh ₃) ₄ Pd; DTPB	2:1	Classical	—	11	—	54

^a The reactions were carried out at 100–110 °C in dry toluene for 24 h (classical heating) or 30 min (microwave irradiation), under N₂, using 0.29 equiv of Pd catalyst and 0.26 equiv of XPhos/DTPB in the presence of 2.1 equiv of KO^tBu.

^b In this reaction two products with lower R_f were isolated in traces amounts. According to the MS spectra, the structures correspond to the bromo derivative with a porphyrinic moiety at the 5-position of indolin-2-one core **8b** (*m/z* 935.9), and to a debrominated porphyrinic compound (*m/z* 858.0).

^c In this reaction the debrominated product was identified as **9a** by detailed NMR analysis and TLC comparison.

yield of the required product (Table 1, entry 8). Finally when tetrakis(triphenylphosphine)palladium(0) was used in an attempt to improve the outcome of the reaction, we were able to isolate **9a** in 81% yield (Table 1, entry 9). It is worth to refer that the reaction of **6** with **8a** under milder Ullmann-type conditions¹⁸ using 5 mol % Cu

Knowing that microwave irradiation could play an important role in the progress of the reaction as evidenced earlier, the coupling of **8b** with **6** was performed using such heating conditions (Table 2, entry 2). The yield of **9b** was improved from 26% to 41%, but no improvement came to **9c**. As in the reaction with **8a**, it was observed

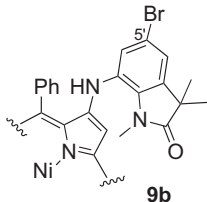
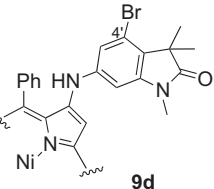
that Ni(II)–2-NH₂–TPP **6** underwent less decomposition. Hoping to obtain the two possible mono-(2-aminoporphyrinyl)- and the di-(2-aminoporphyrinyl)-substituted indolin-2-ones, the ratio of porphyrin/indolin-2-one was changed to 1.5:1 (Table 2, entry 3). It is worth mentioning that such coupling reaction did not give rise to the expected 5-(2-aminoporphyrinyl)-7-bromo-indolin-2-one, and **9b** and **9c** were isolated again (in 28% and 13% yields, respectively). Slight improvement in the yield of **9b** was observed under microwave irradiation using the same reaction conditions (Table 2, entry 4). Aiming to have a higher yield of the bis-product, the 5,7-di-(2-aminoporphyrinyl)-substituted indolin-2-one **9c**, the reaction of

intermediate undergoes debromination to afford the coupled product **9a** (also observed in minor amounts when XPhos was used as ligand).

Afterwards, the reaction of **9b** with 1.5 molar equiv of porphyrin **6** under identical conditions, gave **9c** in 42% yield (Table 3, entry 1). The unreacted Ni(II)–2-NH₂–TPP **6** was recovered (43%) but no **9b** was detected. The same experiment under microwave irradiation (Table 3, entry 2) gave rise to **9c** (10% yield) together with the unreacted porphyrin **6** (59%) and **9b** (51%). This last experiment shows that the microwave assisted heating condition does not promote the 5,7-di-(2-aminoporphyrinyl)-substituted indolin-2-one **9c** formation.

Table 3

Compounds **6/9b,d** ratio and heating condition effects on palladium-catalyzed amination reaction of bromo-indolin-2-one derivatives **9b,d** with Ni(II)–2-NH₂–TPP **6**^a

Entry	6/9b Ratio	Heating	Product yield %		Recovered 6 %	Recovered 9b %	
			9c	9b			
 9b	1	1.5:1	Classical	42	43	—	
	2	1.5:1	MW	10	59	51	
Entry	6/9d Ratio	Heating	Product yield %		Recovered 6 %	Recovered 9d %	
			9e	9f			
 9d	3	2:1	Classical	37	10	53	29

^a The reactions were carried out at 100–110 °C in dry toluene for 24 h (classical heating) or 30 min (microwave irradiation), under N₂, using 0.29 equiv of Pd(OAc)₂ and 0.26 equiv of XPhos in the presence of 2.1 equiv of KO^tBu.

8b with 3 molar equiv of **6** (Table 2, entry 5) was carried out. However, no improvement in the outcome of the reaction was observed: together with **9b** and **9c**, obtained in 14% and 5% yields, respectively, two products with lower *R_f* were isolated in traces amounts. According to the MS spectra, the structures correspond to the bromo-derivative with a porphyrinic moiety at the 5-position of indolin-2-one core **8b** (*m/z* 935.9), and to a debrominated porphyrinic compound (*m/z* 858.0). All these results indicate that the 7'-position, although being more hindered, is more reactive as compared to the 5'-position and this fact supports the higher yield formation of **9b** under these conditions. When we changed the ligand from XPhos to DTPB and carried out the reaction with the ratio of 1.5:1 (porphyrin/indolin-2-one), we observed the formation of compounds **9c** and **9a** in 11 and 18% yields, respectively. Similar results were obtained when the ratio was changed to 2:1 (Table 2, entries 6 and 7). Even when the catalyst was changed to tetrakis(triphenylphosphine)palladium(0) by maintaining the ratio of 2:1 (porphyrin/indolin-2-one) no significant improvement in the yield of compounds **9c** (18%) was observed. Under these conditions the debrominated compound **9a** was isolated as the main product 53% (Table 2, entry 8). Probably under conditions of entries 6–8 in Table 2, the debromination of position **7** in **8b** is an important pathway affording the coupled product **9a** (see theoretical considerations).

It is worthwhile to mention that even on changing the ligand or the catalyst no coupled product having porphyrin moiety at the 5-position of the 5,7-dibromo-indolin-2-one **8b** has been isolated, but instead the debrominated product has been the one obtained. This indicates that the palladium oxidative addition occurs and the

Considering the reaction of Ni(II)–2-NH₂–TPP **6** with 4,6-dibromo substituted indolin-2-one **8c** in a ratio of 1:2 (Table 2, entry 9) it was observed that not only the mono-coupled product 6-(2-aminoporphyrinyl)-4-bromo-indolin-2-one **9d** was formed (44% yield), but also another product identified as being the debrominated 6-(2-aminoporphyrinyl)-indolin-2-one **9e** was obtained (15% yield). In this coupling reaction, the use of microwave irradiation (Table 2, entry 10) led to a significant improvement in the yield of **9d** (63% vs 44%) while **9e** was isolated in a similar yield as the one obtained under classical heating conditions.

Using DTPB and carrying out the reaction under similar conditions (ratio of porphyrin to indolin-2-one; 1:2) as used earlier, there is the selective formation of **9d** in 64% yield (Table 2, entry 11) and no debrominated product **9e** was observed. On changing the ratio of porphyrin to indolin-2-one (2:1) we observed the formation of product **9d** (33%) and another one **9f** (7%); the formation of this latter product implies the entry of porphyrin moiety at the C-4' of the indolin-2-one nucleus (Table 2, entry 12). Also in this case the use of tetrakis(triphenylphosphine)palladium(0) as catalyst gave rise to the formation of products **9d** and **9e** in 23 and 22% yields, respectively (Table 2, entry 13). Another reaction utilizing tetrakis(triphenylphosphine)palladium(0) as the catalyst and DTPB as the ligand led to the formation of product **9e** only (Table 2, entry 14).

Aiming to improve the yield on the porphyrin dyad formation the reaction of the 6-(2-aminoporphyrinyl)-4-bromo-indolin-2-one **9d** with 2 molar equiv of Ni(II)–2-NH₂–TPP **6**, (Table 3, entry 3) has been carried out. Effectively, together with the debrominated **9e** (obtained in 37% yield) and the unreacted porphyrin **6** (53%), a minor

product (10% yield) showing intermediate R_f between the unreacted **9d** (29%) and the **9e** derivative was identified as being the expected 4,6-di-(2-aminoporphyrinyl)-substituted indolin-2-one **9f**.

This last experiment confirms that the palladium-catalyzed debromination competes directly with the attachment of the second porphyrin unit in the 4,6-dibromo-indolin-2-one **8c**. These competitive processes are not uncommon and are being described as side reactions as well as synthetic procedures to afford dehalogenated products.¹⁹

Thinking on the potential use of these compounds in PDT and on the fact that the free bases are capable to generate singlet oxygen, we carried out the decomplexation of one of the new products. In such way compound **9a**, when treated with 10% H_2SO_4 in chloroform, gave rise to the formation of compound **9g** in quantitative yield (Fig. S68 UV–vis spectrum in SI).

2.1. Theoretical considerations

In order to gain insights into the reactivity trends of the 4,6- and 5,7-dibrominated indolin-2-one derivatives (**8c** and **8b**, respectively) towards the amination reactions with Ni(II)–2-NH₂–TPP, theoretical calculations were performed using density-functional theory with the B3LYP functional using Gaussian 03.²⁰ Because of the bulkiness of the porphyrin substituted systems, the Ni(II)–2-NH–TPP substituent was replaced by simple –NH₂ fragments, thus allowing for higher level calculations to be performed, while eliminating conformational dependencies of the

unoccupied molecular orbital (LUMO) of **8b** and **8c**, along with the corresponding aminated models, calculated at the B3LYP/6-311G** level over the optimized geometries at the same level are shown in Fig. 3. In **8b**, and focussing on the halogenated carbon sites, the LUMO is predominantly localized on carbon 7, suggesting that the palladium-catalyzed amination may preferentially occur at that carbon centre since the overlap between the LUMO of **8b** and the HOMO (highest occupied molecular orbital) of the catalyst will be maximized at that site. This result strongly justifies the preferential mono-amination of carbon 7, leading to the formation of compound **9b** (see Table 2, entries 1–5). Once amination takes place at that position, an activation of carbon 5 is observed as the LUMO density becomes higher at that position, thus favouring the formation of the diaminated compound **9c** (see Fig. 4 for the corresponding lowest energy structure). If the first amination were to take place at carbon 5 rather than at carbon 7, an enhancement on the reactivity of position 7 would be observed. However, primary amination at carbon 5 is unlikely to take place as the overlap between the LUMO and HOMO is smaller at that position than that at position 7. An interesting feature of **8b** (which does not occur in **8c**) concerns the phase of the LUMO at both halogenated sites, which is the same in the same side of the ring plane. This suggests that if the catalyst interacts with the indolin-2-one derivative perpendicularly to the molecular plane (which is most likely due to stereochemical hindrance), then the catalyst can easily shift its position towards carbon 7 as to maximize orbital overlap. Hence, amination will only occur at position 5 once position 7 has been aminated.

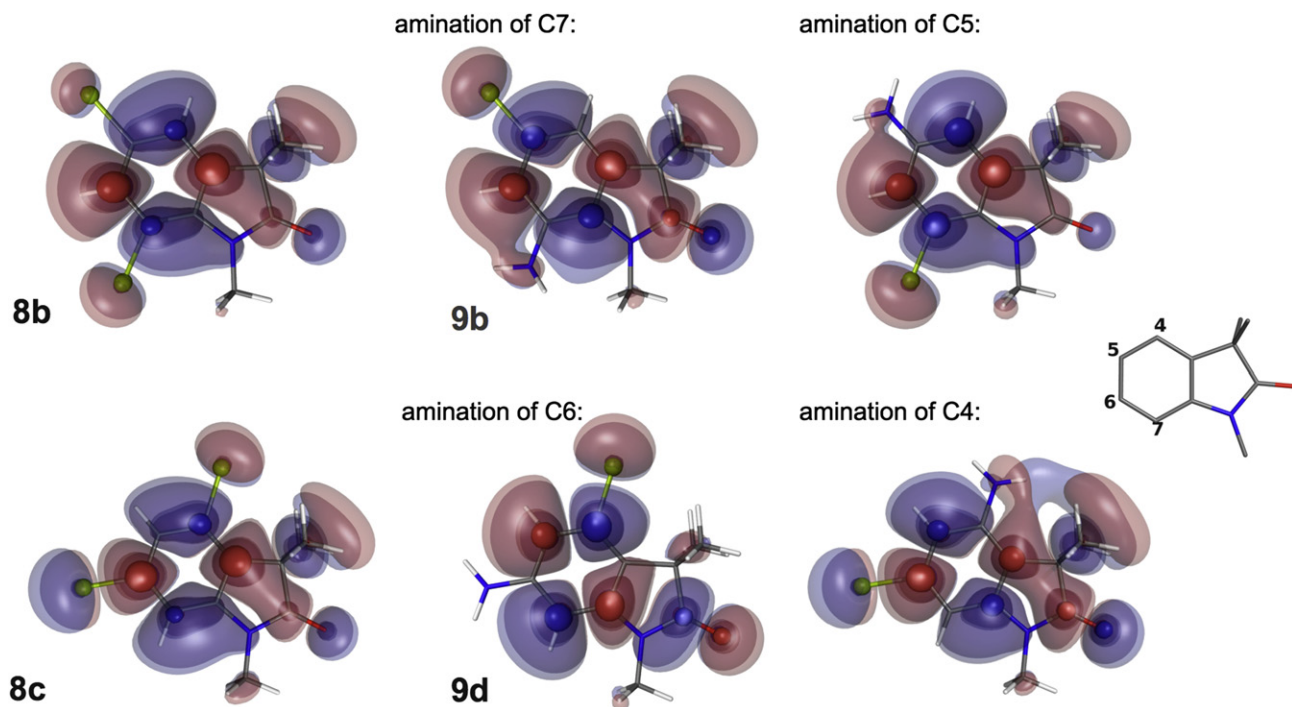


Fig. 3. Depiction of the lowest energy unoccupied molecular orbitals (LUMO, shown at the 0.01, 0.05 and 0.1 au isolevels) of the 5,7- and 4,6-disubstituted indolin-2-ones **8b**, **8c**, **9b** and **9d** (top and bottom rows, respectively), calculated at the B3LYP/6-311G** level; atomic numbering shown for further reference; C, H, N and O depicted in grey, white, blue and red sticks, respectively; Br atoms shown as green spheres.

calculated quantities, which would arise due to the high number of degrees-of-freedom found in the full systems. All calculations were performed in the gas-phase, thus neglecting solvent and catalytic system effects on the reaction mechanism. The following discussion focuses essentially on the Pd(OAc)₂ catalyzed reactions, since these are predominant, hence allowing for trends to be estimated. A similar analysis would be possible for the remaining reactions, although that falls beyond the scope of this paper. The lowest-

Looking into the 4,6-dibrominated compound **8c** (Fig. 3), carbon 6 is expected to be the most reactive halogenated site, as the LUMO is preferentially localized on that carbon. Once amination takes place (leading to **9d**), an increase on the locality of the LUMO on position 4 is observed, similarly to what happens in **8b** upon amination of position 7. Interestingly, the converse is not verified, i.e., primary amination of position 4 does not lead to an increase in the localization of the LUMO in position 6, as it happens analogously in

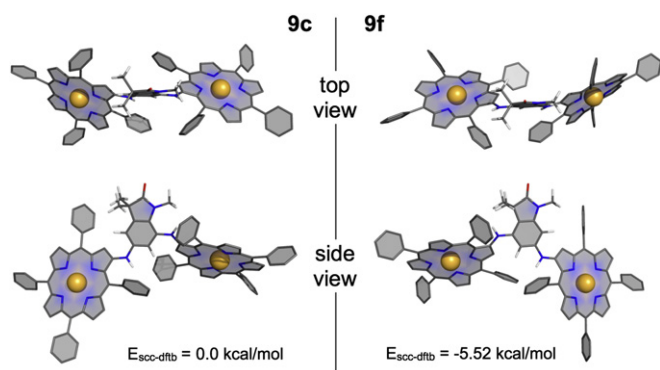


Fig. 4. Lowest energy conformations encountered for the NH–NiTPP disubstituted compounds **9c** and **9f** (left and right, respectively) in the gas-phase, optimized at the scc-dftb level using the DFTB+ code. In both cases, the planar porphyrinic fragments are tilted relatively to the indolin-2-one core due to the stereochemical hindrance from the *meso*-phenyl rings. Hydrogens from the NH–NiTPP fragments were omitted for sake of clarity; colour code as in Fig. 3 (Ni shown as orange spheres).

8b. Hence, amination with Ni(II) porphyrin **6** will preferentially take place at position 6, leading to the formation of **9d**, as it has been found experimentally (secondary amination of position 4 was not significantly observed). The stereochemical hindrance at position 4 due to the two neighbouring methyl groups will probably come into play at this stage, as it may render more difficult the access of the porphyrin **6** to the catalytic centre, thus leading to the debromination of position 4 rather than the formation of the diaminated product. Also, the amination of position 6 leads to major changes in the LUMO, namely in the shape and relative disposition of the nodal surface. This suggests that the secondary amination is only possible if the shape of the LUMO is maintained after the first amination. In fact, the LUMO in **8b** and **8c** are very similar at the beginning (apart from the halogens); upon amination at sites 7 and 6, respectively (leading to **9b** and **9d**, respectively), only the LUMO of **9b** maintains its essential form, hence rendering the second amination possible. This orbital shape preconditioning will probably be a requirement of the catalyst, whose HOMO may not otherwise efficiently overlap the LUMO of **9d** (this hypothesis was not evaluated). If such is the case, and along with the possible stereochemical hindrance from both methyl groups in position 3, the debromination of position 4 in **9d** may be favoured, thus leading to the formation of compound **9e**.

The localization of the LUMO also seems to play an important role in the reactivity of the mono-iodinated compound **8a** (Fig. 5). In this case, the lowest energy unoccupied orbital is negligibly centred on carbon 5, leading to low reactivities of that site towards amination, as it has also been found experimentally (Table 1; entries 1–8). Nevertheless, attention must be paid to the nature and

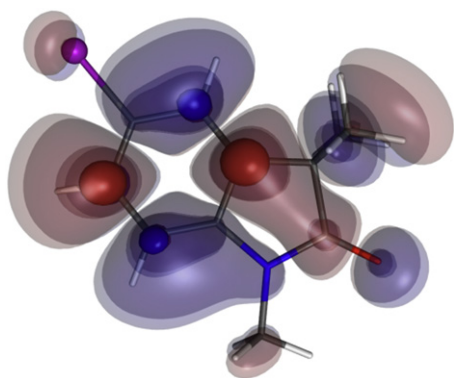


Fig. 5. Depiction of the LUMO of compound **8a** (details as in Fig. 3; iodine atom shown as purple sphere).

size of the catalytic system, which will largely influence the outcome of the reactions. For instance, in entry 9 from Table 1 (reaction of **8a** with $(\text{PPh}_3)_4\text{Pd}$; XPhos), the shape of the HOMO of the catalytic system may allow for bigger overlaps, thus increasing the reaction yield (hypothesis not evaluated), whereas in entry 8 from Table 2 (similar reaction with **8b**), the bulkiness of the catalyst system may render it more difficult to access the reaction site due to stereochemical hindrance from the nearby *N*-methyl group.

2.2. Characterization of new compounds

The ^1H NMR spectrum of compound **9a** was in agreement with the proposed structure showing a singlet for six protons at 1.34 ppm due to the C-3' *gem*-dimethyl group of the indolin-2-one nucleus, and another singlet at 3.20 ppm for the *N*-methyl group. A singlet was also observed for the porphyrin β -NH proton at 6.21 ppm, which was identified by H/D exchange with D_2O . The resonances of the aromatic protons of the indolin-2-one ring were assigned as a multiplet at 6.70–6.71 ppm for H-6' and H-7' and a doublet at 7.11 ppm (J 1.6 Hz) for H-4'. The proton resonances of the porphyrin moiety were observed as multiplets in the region 7.60–7.79 ppm for those at the *meta* and *para* positions, and at 7.93–8.00 ppm for the ones at *ortho* positions of the *meso*-phenyl groups. The signal for the resonance of the H-3 of the porphyrin moiety was observed as a singlet at 8.06 ppm, while in the region between 8.54 and 8.69 ppm are found the signals (one doublet with J 4.9 Hz and a multiplet) corresponding to the resonances of the remaining β -pyrrolic protons. The structure of **9a** was further confirmed by 2D COSY, HSQC and HMBC experiments, which showed the correlation of the NH proton signal with the signals of carbon C-3 of the porphyrinic ring (109.3 ppm) and C-4' (112.7 ppm) and C-6' (116.6 ppm) of the indolin-2-one (see the main HMBC correlations in Fig. 6).

The HRMS spectrum of **9b** showed a peak at m/z 936.1710 corresponding to the M^{++} ion and the ^1H NMR data presented the resonances due to the porphyrin unit with a similar pattern to the one described for compound **9a**. The resonances of the two aromatic protons of the indolin-2-one moiety appearing as two doublets (H-4' at 7.12 ppm and H-6' at 7.24 ppm) with a J 1.9 Hz, indicating the *meta* substituted position relatively to each other. The linkage position was determined by 2D NMR studies including HMBC wherein the signal of the NH proton attached to the porphyrin (a singlet at 5.72 ppm) as well as those of the two aromatic protons H-4' and H-6' correlate with that of the quaternary carbon C-7'a (136.0 ppm). The proton signal of the *N*-methyl group of the indolin-2-one moiety (3.19 ppm) also show correlation with the same quaternary carbon confirming that the 2-aminoporphyrin ring is attached to the C-7'- and not to the C-5' (see the main HMBC correlations in Fig. 6). The HRMS spectrum of **9c** exhibits the peak at m/z 1541.4226 corresponding to the insertion of two 2-aminoporphyrin units into the indolin-2-one core. The ^1H NMR spectrum shows two singlets at 5.78 and 6.17 ppm that do not present any correlation with proton or carbon signals in the COSY and HSQC spectra. As a result, these two signals correspond to the resonance of the NH proton attached to each porphyrinic unit. While the signal at 5.78 ppm correlates, in the HMBC (see Fig. 6), with the carbon signal at 110.8 ppm, the singlet at 6.17 ppm correlates with the same carbon and the one appearing at 109.2 ppm. The correlations found in the HSQC spectrum and the multiplicity (doublet) and respective coupling constant (J 2.1 Hz) of the corresponding proton signals at 7.00 and 6.54 ppm allowed us to assign them to the resonances of H-6' and H-4', respectively. Therefore, the singlet at 5.78 ppm corresponds to the resonance of NH proton of the 2-aminoporphyrin ring attached to the C-7', and the one at 6.17 ppm to the NH of the porphyrinic macrocycle at C-5'. Moreover, the H-6' and H-4' signals as well as the one due to the NH of

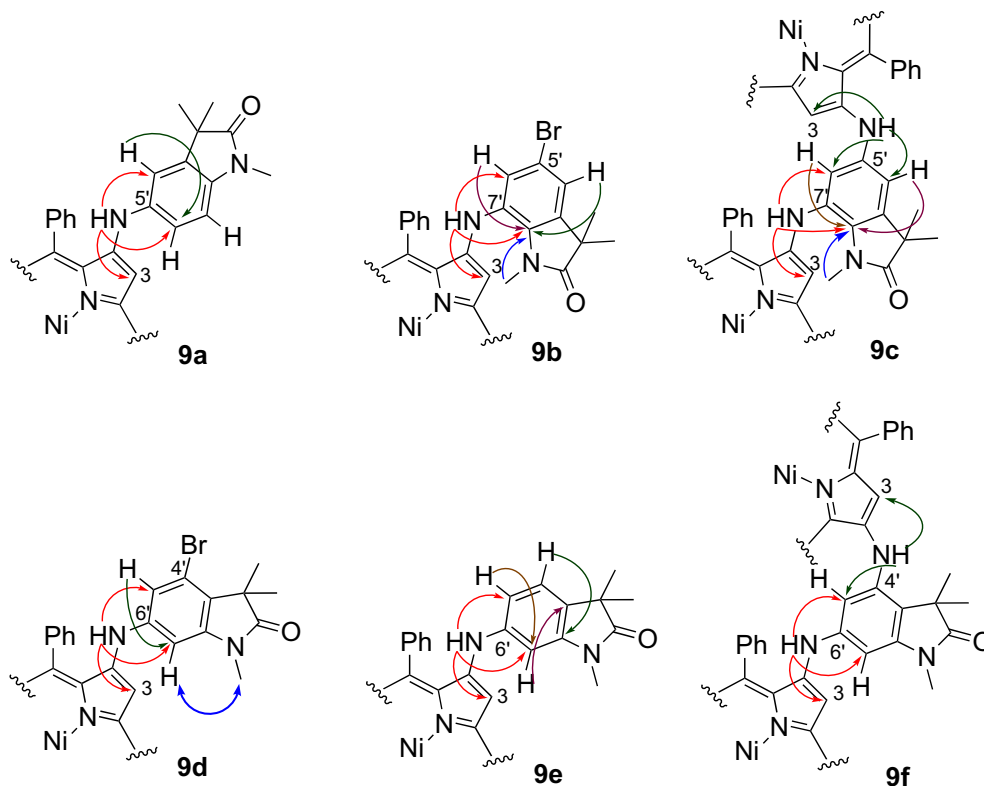


Fig. 6. Structures, main HMBC and NOESY correlations of synthesized mono-(2-aminoporphyrinyl)- and di-(2-aminoporphyrinyl)-substituted indolin-2-ones **9a–f**.

the porphyrin at C-7' and the protons of the *N*-methyl group (3.19 ppm) correlate with the quaternary carbon C-7'a (129.8 ppm).

The ^1H NMR spectra of **9d** and **9e** showed a similar substitution pattern to the ones observed for **9b** and **9a**, respectively. In the case of **9d**, the NOESY spectrum showed a correlation between the signal of the *N*-methyl group (a singlet at 3.11 ppm) and the doublet at 6.64 ppm (J 1.9 Hz) corresponding to the resonance of H-7'. Consequently, the linkage position in the monobromo derivative **9d** was confirmed to be at the C-6' of the indolin-2-one ring by HMBC (Fig. 6), wherein, a correlation was seen between the signal of the NH proton (6.32 ppm) with those of C-7' and C-5' carbons (95.3 and 113.8 ppm, respectively). This fact indicates that after formation of **9d**, it undergoes debromination under the reaction conditions to form **9e**. This is supported by the ^1H NMR pattern of **9e** with respect to the aromatic part of the indolin-2-one ring where the presence of the doublet of doublets at 6.31 ppm (J 2.0 and 7.9 Hz, H-5') and the two doublets at 6.77 ppm (J 2.0 Hz, H-7') and 7.03 ppm (J 7.9 Hz, H-4') can only be justified if the porphyrin is linked at the 6-position of this unit. The HMBC correlations (Fig. 6) are consistent with the proposed structure **9e**. These results were confirmed by the HRMS data of compounds **9d** and **9e**, which showed peaks at m/z 936.1702 and 858.2612, respectively.

The HRMS spectrum of **9f** showed a peak at m/z 1542.4356 corresponding to the $(\text{M}+\text{H})^+$ ion¹⁵ and the ^1H NMR data was in accord with the proposed structure. In the HMBC spectrum (see the main correlations in Fig. 6) the signal of the NH proton of the 2-aminoporphyrin attached to the C-6' (assigned as a singlet at 6.38 ppm) correlates with the carbon signals at 92.4 and 100.6 ppm attributed to C-7' and C-5', respectively. This last signal is also correlating with the singlet at 5.97 ppm corresponding to the resonance of the NH proton of the porphyrinic macrocycle in the C-4'. Moreover, the signals attributed to the proton resonances of the *N*-methyl group (singlet at 3.15 ppm), H-7' (doublet, J 1.5 Hz, at 5.92 ppm) and H-5' (doublet, J 1.5 Hz, at 7.47 ppm) correlate with the quaternary carbons C-7'a (144.84 ppm) and C-3'a (115.9 ppm).

Compound **9g** showed the inner N–H of the macrocycle at -2.53 ppm thus indicating the removal of Ni metal ion while other peaks were similar to those observed in the complexed form; the free base structure was also confirmed by its HRMS at m/z 803.3479 for its $(\text{M}+\text{H})^+$ ion.¹⁵

3. Conclusion

In summary, a series of mono-(2-aminoporphyrinyl)- and di-(2-aminoporphyrinyl)-indolin-2-one conjugates were synthesized by reactions of 5-iodo; 4,6- and 5,7-dibrominated indolin-2-one derivatives with (2-amino-5,10,15,20-tetraphenylporphyrinato)nickel(II) via Buchwald–Hartwig palladium-catalyzed aminations supported by a phosphine ligand. These studies demonstrated that the efficiency and course of the coupling process depend on various factors like the used catalytic system, the number and position of the halogen substituent and heating condition. Theoretical calculations provide insights into the reactivity of the iodo and dibrominated indolin-2-one derivatives. Using these synthetic methods, we are currently working to construct libraries of porphyrins for potential applications in medicine.

4. Experimental section

4.1. General

The microwave heating amination reactions were performed with an Ethos SYNTH microwave labstation (Milestone) using a closed glass reactor (temperature measurement with a fibre-optic probe and Weflon™ bar along with magnetic stirring). ^1H NMR spectra were recorded at 300 or 500 MHz and ^{13}C NMR spectra were recorded at 75.5 or 125.8 MHz with Bruker Avance 300 and Bruker DRX 500 spectrometers. CDCl_3 was used as solvent. Chemical shifts (δ) are expressed in parts per million (ppm) relative to tetramethylsilane. The coupling constants (J) are given in hertz

(Hz). Unequivocal ^1H assignments were made using 2D COSY and NOESY experiments (mixing time of 800 ms) while ^{13}C assignments were made on the basis of DEPT-135 and 2D HSQC and HMBC experiments (delay for long-range $J\text{C}/\text{H}$ couplings were optimized for 7 Hz). The HRMS (ESI) were determined with a Bruker Apex-Qe spectrometer using chloroform as solvent and 3-nitrobenzyl alcohol (NBA) as matrix. The UV–vis spectra were recorded with a Shimadzu UV-250 Pc spectrophotometer using chloroform as solvent (1 cm path length quartz cell). Melting points were measured with a Büchi B-540 melting point apparatus and are uncorrected. Preparative thin layer chromatography was carried out on 20×20 cm glass plates coated with silica gel (1 mm thick, Merck). Analytical TLC was carried out on precoated sheets with silica gel (0.2 mm thick, Merck). Dichloromethane was distilled from calcium hydride, and toluene was dried over sodium metal. All other solvents and reagents were used without further purification.

(2-Amino-5,10,15,20-tetraphenylporphyrinato)nickel(II)¹¹ **6** and indolin-2-one derivatives **7a–c**¹² were prepared according to known procedures and were characterized by comparing its ^1H NMR spectrum to the previously reported data. The 5-iodo-1,3,3-trimethylindolin-2-one¹⁴ **8a** and (2-phenylamino-5,10,15,20-tetraphenylporphyrinato)nickel(II)^{3f} **10** are also described and were characterized by comparing their ^1H NMR and MS spectra to the previously reported data.

4.2. General procedure for the N-methylation reaction¹³ of indolin-2-ones **7a–c**

5-Iodo-indolin-2-one **7a** (50 mg, 193 μmol) and methyl iodide (72.1 μL , 1.16 mmol, 6 equiv) were added to a vigorously stirred solution of KOH (45.1 mg, 0.80 mmol, 4 equiv) in DMSO (2 mL) at room temperature. The reaction was monitored by TLC until complete consumption of **7a** (30 min). After water addition, the reaction mixture was extracted with ethyl acetate and the organic layer dried over Na_2SO_4 . Solvent was then evaporated under reduced pressure and the 5-iodo-1,3,3-trimethylindolin-2-one **8a** was purified using preparative thin layer chromatography [light petroleum/ethyl acetate (3:2)]. Crystallization from dichloromethane/light petroleum afforded **8a** in 74% yield (43 mg).

4.2.1. 5-Iodo-1,3,3-trimethylindolin-2-one¹⁴ **8a**. HRMS (ESI) m/z calcd for $\text{C}_{11}\text{H}_{13}\text{INO}$ ($\text{M}+\text{H}$)⁺ 302.0036, found 302.0036.

4.2.2. 5,7-Dibromo-1,3,3-trimethylindolin-2-one **8b**. Yield: 79% (45 mg); yellow solid; mp 125–127 °C (CH_2Cl_2 /light petroleum); δ_{H} (300 MHz, CDCl_3) 1.36 (s, 6H, $\text{CH}_3 \times 2$), 3.57 (s, 3H, NCH_3), 7.22 (d, 1H, J 2.0 Hz, H-4), 7.52 (d, 1H, J 2.0 Hz, H-6); δ_{C} (75 MHz, CDCl_3) 24.5 ($\text{CH}_3 \times 2$); 29.7 (NCH_3); 44.2 (C-3); 102.7 (C-7); 115.3 (C-5); 124.7 (C-4); 135.1 (C-6); 139.3 (C-7a); 140.4 (C-3a); 181.0 (C-2); HRMS (ESI) m/z calcd for $\text{C}_{11}\text{H}_{12}\text{Br}_2\text{NO}$ ($\text{M}+\text{H}$)⁺ 331.9280, found 331.9279.

4.2.3. 4,6-Dibromo-1,3,3-trimethylindolin-2-one **8c**. Yield: 70% (39.8 mg); brownish oil; δ_{H} (300 MHz, CDCl_3) 1.50 (s, 6H, $\text{CH}_3 \times 2$), 3.19 (s, 3H, NCH_3), 6.93 (d, 1H, J 1.5 Hz, H-7), 7.33 (d, 1H, J 1.5 Hz, H-5); δ_{C} (75 MHz, CDCl_3) 21.2 ($\text{CH}_3 \times 2$); 26.4 (NCH_3); 46.2 (C-3); 110.6 (C-7); 119.0 (C-4); 121.7 (C-6); 128.7 (C-5); 132.2 (C-3a); 145.6 (C-7a); 180.5 (C-2); HRMS (ESI) m/z calcd for $\text{C}_{11}\text{H}_{12}\text{Br}_2\text{NO}$ ($\text{M}+\text{H}$)⁺ 331.9280, found 331.9279.

4.3. General procedures for the reaction of (2-amino-5,10,15,20-tetraphenylporphyrinato)nickel(II) **6** with 1,3,3-trimethylindolin-2-ones **8a–c** under Buchwald conditions

Procedure (i) Classical heating: In an oven dried Schlenck tube, purged with N_2 , porphyrin **6** (14.5 μmol) and 1,3,3-trimethylindolin-2-ones **8a–c** (29.2 μmol , 2 equiv) were dissolved

in dry, degassed toluene (5 mL). To this solution were added $\text{Pd}(\text{OAc})_2/(\text{PPh}_3)_4\text{Pd}$ (4.2 μmol , 0.29 equiv), ligand (3.8 μmol , 0.26 equiv) and KO^tBu (30.3 μmol , 2.1 equiv). The mixture was kept under a nitrogen atmosphere for 24 h at 100–110 °C. After cooling to room temperature and addition of chloroform, the reaction mixture was filtered through a short plug column of Celite[®]-545 and washed several times with water. The organic layer was dried over Na_2SO_4 . After evaporation of the solvents under reduced pressure, the solid residue was taken up in CHCl_3 and then purified by preparative thin layer chromatography [light petroleum/chloroform (1:2)]. The first eluted fraction was the starting material Ni(II)–2-NH₂–TPP **6**. Then, the desired (2-aminoporphyrinyl)-indolin-2-ones **9a–f** were isolated after crystallization from chloroform/methanol.

Procedure (ii) Microwave heating: In a closed glass reactor, purged with N_2 , porphyrin **6** (14.5 μmol) and 1,3,3-trimethylindolin-2-ones **8a–c** (29.2 μmol , 2 equiv) were dissolved in dry, degassed toluene (2.5 mL). To this solution were added $\text{Pd}(\text{OAc})_2$ (4.2 μmol , 0.29 equiv), XPhos (3.8 μmol , 0.26 equiv) and KO^tBu (30.3 μmol , 2.1 equiv). The vessel was placed inside the centre of the microwave oven and then was exposed to microwave irradiation for 30 min (800 W for 2 min to reach 110 °C and 500 W to maintain the reflux). After irradiation, the reaction mixture was cooled to room temperature, filtered through a short plug column of Celite[®]-545 (using chloroform) and washed with water. The organic layer was dried over Na_2SO_4 and the solvent removed under reduced pressure. Further purification by preparative thin layer chromatography, using a mixture of light petroleum/chloroform (1:2), afforded the starting material Ni(II)–2-NH₂–TPP **6**, and the desired (2-aminoporphyrinyl)-indolin-2-ones **9a–f** by crystallization from chloroform/methanol.

4.3.1. 5-[(2-Amino-5,10,15,20-tetraphenylporphyrinato)nickel(II)]-1,3,3-trimethylindolin-2-one **9a**. δ_{H} (300 MHz, CDCl_3) 1.34 (s, 6H, $\text{CH}_3 \times 2$), 3.20 (s, 3H, NCH_3), 6.21 (s, 1H, NH), 6.69 (dd, 1H, J 8.2, 2.0 Hz, H-6'), 6.73 (d, J 8.2 Hz, 1H, H-7'), 7.11 (d, 1H, J 1.6 Hz, H-4'), 7.60–7.79 (m, 12H, H-*m,p*-Ph), 7.93–8.00 (m, 8H, H-*o*-Ph), 8.06 (s, 1H, H-3), 8.54 (d, 1H, J 4.9 Hz, H- β), 8.62–8.69 (m, 5H, H- β); δ_{C} (125 MHz, CDCl_3) 24.3 ($\text{CH}_3 \times 2$); 26.3 (NCH_3); 44.4 (C-3'); 108.4 (C-7'); 109.3 (C-3); 112.7 (C-4'); 115.5, 115.6; 116.6 (C-6'); 118.4, 120.2; 126.86, 126.89, 126.94, 127.5, 127.6, 127.7, 128.5, 128.8 (C-*m,p*-Ph); 130.4, 131.3, 131.4, 131.7, 131.8, 132.9 (C- β); 132.5, 133.4, 133.5, 133.6 (C-*o*-Ph); 136.8 and 137.0 (C-7'a and C-3'a); 137.9 (C-5'); 139.6, 140.8, 140.9, 141.2, 141.3, 142.1, 142.8, 142.9, 143.1, 143.7, 147.6; 181.0 (C-2'); UV–vis (CHCl_3): λ_{max} (log ϵ) 414 (5.13), 540 (4.12), 586 (4.21) nm; HRMS (ESI) m/z calcd for $\text{C}_{55}\text{H}_{40}\text{N}_6\text{NiO}$ (M^+) 858.2611, found 858.2611.

The results of all these experiments are summarized in Tables 1 and 2.

4.3.2. 7-[(2-Amino-5,10,15,20-tetraphenylporphyrinato)nickel(II)]-5-bromo-1,3,3-trimethylindolin-2-one **9b**. δ_{H} (300 MHz, CDCl_3) 1.36 (s, 6H, $\text{CH}_3 \times 2$), 3.19 (s, 3H, NCH_3), 5.72 (s, 1H, NH), 7.12 (d, 1H, J 1.9 Hz, H-4'), 7.24 (d, 1H, J 1.9 Hz, H-6'), 7.39 (s, 1H, H-3), 7.54–7.77 (3 m, 12H, H-*m,p*-Ph), 7.84–8.03 (2m, 8H, H-*o*-Ph), 8.56 (d, 1H, J 4.9 Hz, H- β), 8.58 (d, 1H, J 4.9 Hz, H- β), 8.65–8.71 (m, 4H, H- β); δ_{C} (75 MHz, CDCl_3) 24.6 ($\text{CH}_3 \times 2$); 28.4 (NCH_3); 44.1 (C-3'); 110.6 (C-3); 115.0 (C-5'); 115.8, 116.0, 118.59, 118.65, 120.2; 122.7 (C-4'); 126.9, 127.0, 127.5, 127.7, 127.76, 128.5, 129.2 (C-*m,p*-Ph); 127.83 (C-6'); 130.6, 131.5, 131.6, 131.9, 132.2, 132.9 (C- β and C-*o*-Ph); 133.47, 133.56, 133.65 (C-*o*-Ph); 136.0 (C-7'a); 139.4; 139.9 (C-3'a); 127.3, 131.7, 140.7, 140.9, 141.2, 141.5, 142.2, 142.7, 142.8, 142.9, 143.1, 150.5; 181.4 (C-2'); UV–vis (CHCl_3): λ_{max} (log ϵ) 416 (5.09), 540 (4.02), 582 (3.91) nm; HRMS (ESI) m/z calcd for $\text{C}_{55}\text{H}_{39}\text{BrN}_6\text{NiO}$ (M^+) 936.1717, found 936.1710.

4.3.3. 5,7-Bis[(2-amino-5,10,15,20-tetraphenylporphyrinato)nickel(II)]-1,3,3-trimethylindolin-2-one **9c**. δ_{H} (300 MHz, CDCl_3) 1.36 (s, 6H, $\text{CH}_3 \times 2$), 3.19 (s, 3H, NCH_3), 5.78 (s, 1H, NH of porphyrin at C-7'),

6.17 (s, 1H, NH of porphyrin at C-5'), 6.54 (d, 1H, *J* 2.1 Hz, H-4'), 6.55–6.59 (m, 1H, H-*m*-Ph), 6.71–6.75 (m, 1H, H-*m*-Ph), 7.00 (d, 1H, *J* 2.1 Hz, H-6'), 7.02–7.07 (m, 1H, H-*m*-Ph), 7.21 (t, 1H, *J* 7.5 Hz, H-*m*-Ph), 7.48 (s, 1H, H-3 of porphyrin at C-7'), 7.56–7.71 (m, 24H, 4 20-H-*o*-Ph and 20 H-*m,p*-Ph), 7.91–8.04 (m, 12H, H-*o*-Ph), 8.09 (s, 1H, H-3 of porphyrin at C-5'), 8.41 (d, 1H, *J* 5.0 Hz, H-β), 8.44 (d, 1H, *J* 5.0 Hz, H-β), 8.53–8.74 (m, 10H, H-β); δ_C (125 MHz, CDCl₃) 24.7 (CH₃ × 2); 28.4 (NCH₃); 44.1 (C-3'); 109.2 (C-4'); 110.7 (C-3 of porphyrin at C-7'); 110.8 (C-6'); 111.5 (C-3 of porphyrin at C-5'); 115.7, 115.8, 115.9, 118.46, 118.48, 120.21, 120.24, 126.5, 126.89, 126.91, 127.67; 126.4, 126.7, 126.87, 127.1, 127.2, 127.64, 127.74, 127.77, 128.4, 128.5, 128.6, 129.1 (C-*m,p*-Ph); 129.8 (C-7'a); 130.46, 130.51, 131.4, 131.5, 131.7, 131.91, 131.96, 132.0, 132.3, 132.5, 132.8, 132.9 (C-β); 133.0, 133.3, 133.5, 133.6, 133.7 (C-*o*-Ph); 138.4; 139.2 (C-3'a); 139.5, 139.6, 140.69, 140.72, 140.75, 141.01, 141.03, 141.45, 141.48, 142.1, 142.81, 142.86, 142.88, 142.91, 143.1, 143.2, 143.3, 146.1, 150.6; 181.5 (C-2'); UV-vis (CHCl₃): λ_{\max} (log ϵ) 414 (5.34), 538 (4.26), 588 (4.30) nm; HRMS (ESI) *m/z* calcd for C₉₉H₆₇N₁₁Ni₂O (M⁺) 1541.4231, found 1541.4226.

4.3.4. 6-[(2-Amino-5,10,15,20-tetraphenylporphyrinato)nickel(II)]-4-bromo-1,3,3-trimethylindolin-2-one **9d**. δ_H (300 MHz, CDCl₃) 1.50 (s, 6H, CH₃ × 2), 3.11 (s, 3H, NCH₃), 6.32 (s, 1H, NH), 6.47 (d, 1H, *J* 1.9 Hz, H-5'), 6.64 (d, 1H, *J* 1.9 Hz, H-7'), 7.63–7.83 (2m, 12H, H-*m,p*-Ph), 7.96–8.01 (m, 8H, H-*o*-Ph), 8.26 (s, 1H, H-3), 8.58 (d, 1H, *J* 5.0 Hz, H-β), 8.66–8.72 (m, 5H, H-β); δ_C (75 MHz, CDCl₃) 21.8 (CH₃ × 2); 26.1 (NCH₃); 46.0 (C-3'); 95.3 (C-7'); 112.9 (C-3); 113.8 (C-5'); 115.7, 116.2; 118.7, 118.8 (C-4' and C-6'); 120.2; 124.9 (C-3'a); 126.90, 126.92, 127.0, 127.7, 127.8, 128.6, 128.9 (C-*m,p*-Ph); 130.8, 131.6, 131.9, 132.0, 132.4 (C-β); 132.99, 133.03, 133.4, 133.5, 133.6 (C-*o*-Ph); 139.5, 140.62, 140.65, 141.1, 141.3, 141.7, 142.3, 142.8, 142.9, 143.3, 144.7; 145.2 (C-7'a); 181.3 (C-2'); UV-vis (CHCl₃): λ_{\max} (log ϵ) 418 (5.02), 544 (3.97), 580 (4.01) nm; HRMS (ESI) *m/z* calcd for C₅₅H₃₉BrN₆NiO (M⁺) 936.1717, found 936.1702.

4.3.5. 6-[(2-Amino-5,10,15,20-tetraphenylporphyrinato)nickel(II)]-1,3,3-trimethylindolin-2-one **9e**. δ_H (300 MHz, CDCl₃) 1.36 (s, 6H, CH₃ × 2), 3.14 (s, 3H, NCH₃), 6.31 (dd, 1H, *J* 2.0, 7.9 Hz, H-5'), 6.44 (s, 1H, NH), 6.77 (d, 1H, *J* 2.0 Hz, H-7'), 7.03 (d, 1H, *J* 7.9 Hz, H-4'), 7.61–7.82 (2m, 12H, H-*m,p*-Ph), 7.97–8.00 (m, 8H, H-*o*-Ph), 8.25 (s, 1H, H-3), 8.56 (d, 1H, *J* 5.0 Hz, H-β), 8.65–8.71 (m, 5H, H-β); δ_C (75 MHz, CDCl₃) 24.5 (CH₃ × 2); 26.0 (NCH₃); 43.9 (C-3'); 96.5 (C-7'); 110.4 (C-5'); 111.0 (C-3); 115.4, 116.8, 119.9, 122.4; 122.9 (C-4'); 127.9 (C-3a'); 126.9, 127.0, 127.7, 127.8, 128.5, 128.9 (C-*m,p*-Ph); 130.6, 131.5, 131.8, 132.5, 132.9 (C-β); 133.4, 133.5, 133.6 (C-*o*-Ph); 133.0, 136.9, 138.9, 140.0, 140.3, 140.7, 141.2, 141.5, 142.2, 143.0; 143.6 (C-7'a); 145.9; 182.0 (C-2'); UV-vis (CHCl₃): λ_{\max} (log ϵ) 416 (5.02), 542 (3.97), 582 (4.01) nm; HRMS (ESI) *m/z* calcd for C₅₅H₄₀N₆NiO (M⁺) 858.2611, found 858.2612.

4.4. General procedures for the reaction (2-amino-5,10,15,20-tetraphenylporphyrinato)nickel(II) **6** with bromo-indolin-2-ones **9b,d** under Buchwald conditions

Procedure (iii) Classical heating: In an oven dried Schlenk tube, purged with N₂, 7-(2-aminoporphyrinyl)-5-bromo-indolin-2-one **9b** (6.1 μmol) and Ni(II)–2-NH₂–TPP **6** (9.1 μmol, 1.5 equiv) were dissolved in dried, degassed toluene (5 mL). To this solution were added Pd(OAc)₂ (1.8 μmol, 0.29 equiv), XPhos (1.7 μmol, 0.28 equiv) and KO^tBu (12.7 μmol, 2.1 equiv). The mixture was kept under a nitrogen atmosphere for 24 h at 100–110 °C. After cooling to room temperature and addition of chloroform, the reaction mixture was filtered through a short plug column of Celite[®]-545 and washed several times with water. The organic layer was dried over Na₂SO₄. After evaporation of the solvents under reduced pressure, the solid residue was taken up in CHCl₃ and then purified by preparative thin

layer chromatography [light petroleum/chloroform (1:2)]. The starting material Ni(II)–2-NH₂–TPP **6** and the 5,7-di-(2-aminoporphyrinyl)-substituted indolin-2-one **9c** were crystallized from chloroform/methanol.

Procedure (iv) Microwave heating: In a closed glass reactor, purged with N₂, porphyrin **9b** (11.8 μmol) and Ni(II)–2-NH₂–TPP **6** (17.9 μmol, 1.5 equiv) were dissolved in dry, degassed toluene (5 mL). To this solution were added Pd(OAc)₂ (4.2 μmol, 0.29 equiv), XPhos (3.1 μmol, 0.26 equiv) and KO^tBu (24.9 μmol, 2.1 equiv). Similar microwave program was utilized as mentioned earlier. After irradiation, the reaction mixture was cooled to room temperature, filtered through a short plug column of Celite[®]-545 (using chloroform) and washed with water. The organic layer was dried over Na₂SO₄ and the solvent removed under reduced pressure. Further purification by preparative thin layer chromatography, using a mixture of light petroleum/chloroform (1:2), afforded the starting material **6**, **9b** and **9c**. All compounds were crystallized from chloroform/methanol.

The results of all these experiments are summarized in Table 3.

4.4.1. 4,6-Bis[(2-amino-5,10,15,20-tetraphenylporphyrinato)nickel(II)]-1,3,3-trimethylindolin-2-one **9f**. δ_H (300 MHz, CDCl₃) 1.11 (s, 6H, CH₃ × 2), 3.15 (s, 3H, NCH₃), 5.92 (d, 1H, *J* 1.5 Hz, H-7'), 5.97 (s, 1H, NH of porphyrin at C-4'), 6.25–6.35 (m, 2H, H-*m*-Ph), 6.38 (s, 1H, NH of porphyrin at C-6'), 6.57 (t, 1H, *J* 7.3 Hz, H-*m*-Ph), 6.87 (t, 1H, *J* 7.3 Hz, H-*m*-Ph), 7.36–7.42 (m, 4H, 20-H-*o*-Ph), 7.47 (d, 1H, *J* 1.5 Hz, H-5'), 7.54–7.70 (m, 20H, H-*m,p*-Ph), 7.92–8.05 (m, 12H, H-*o*-Ph), 7.95 (s, 1H, H-3 of porphyrin at C-4'), 8.23 (s, 1H, H-3 of porphyrin at C-6'), 8.32–8.74 (m, 12H, H-β); δ_C (75 MHz, CDCl₃) 22.9 (CH₃ × 2); 26.2 (NCH₃); 43.9 (C-3'); 92.4 (C-7'); 100.6 (C-5'); 113.0 (C-3 of porphyrin at C-4'); 113.37 (C-3 of porphyrin at C-6'); 113.43, 115.7; 115.9 (C-3'a); 118.4, 120.2, 124.5, 126.8, 126.93, 127.12, 127.9, 129.0, 131.7, 133.2; 126.2, 126.5, 126.89, 127.15, 127.6, 127.8, 128.5, 128.6 (C-*m,p*-Ph); 130.7, 131.5, 131.8, 131.9, 132.0, 132.5, 132.6, 132.8 (C-β); 133.4, 133.59, 133.65, 133.67 (C-*o*-Ph); 139.57, 139.60, 139.7, 140.5, 140.6, 140.7, 141.1, 141.6, 142.1, 142.6, 142.81, 142.85, 142.9, 143.0, 143.2, 143.5, 144.79; 144.84 (C-7'a); 148.3; 181.5 (C-2'); UV-vis (CHCl₃): λ_{\max} (log ϵ) 416 (5.34), 544 (4.66), 585 (4.49) nm; HRMS (ESI) *m/z* calcd for C₉₉H₆₈N₁₁Ni₂O (M+H)⁺ 1542.4310, found 1542.4356.

4.4.2. Demetallation of compound **9a** to 5-[2-Amino-5,10,15,20-tetraphenylporphyrin]-1,3,3-trimethylindolin-2-one **9g**. Porphyrin **9a** (7.33 μmol) was treated with a mixture of 10% H₂SO₄ in chloroform (10 mL). The reaction mixture was stirred at room temperature for 2 min and then neutralized with a saturated solution of NaHCO₃. The aqueous phase was extracted with chloroform, and the organic phase was dried over Na₂SO₄ and evaporated in vacuum to dryness. The resulting residue was purified by preparative TLC. δ_H (300 MHz, CDCl₃) –2.54 (s, 2H, NH), 1.37 (s, 6H, CH₃ × 2), 3.22 (s, 3H, NCH₃), 6.43 (s, 1H, NH), 6.72 (dd, 1H, *J* 8.3, 1.9 Hz, H-6'), 6.77 (d, 1H, *J* 8.3, 1.9 Hz, H-7'), 7.29 (d, 1H, *J* 1.9 Hz, H-4'), 7.68–7.89 (m, 12H, H-*m,p*-Ph), 8.11 (s, 1H, H-3), 8.15–8.23 (m, 8H, H-*o*-Ph), 8.55 (d, 1H, *J* 4.8 Hz, H-β), 8.73–8.82 (m, 5H, H-β); UV-vis (CHCl₃): λ_{\max} (log ϵ) 410 (5.33), 523 (4.39), 574 (4.24), 602 (4.22), 657 (3.97) nm; HRMS (ESI) *m/z* calcd for C₅₅H₄₃N₆O (M+H)⁺ 803.3498, found 803.3479.

4.5. Theoretical calculations

Theoretical calculations were performed using density-functional theory, with Gaussian 03.²⁰ Molecular geometries were optimized using the B3LYP functional with the 6-311G** basis-set, having all properties been calculated at the same level over the optimized structures. Conformational analysis of **9c** and **9f** was performed at the scc-dftb level using DFTB+,² with parameters taken from the mio-0-1²¹ and trans3d-0-1²² sets (for {C, H, N, O}) and

{Ni}, respectively); default program parameters were used in the geometry optimization steps; geometries were considered converged once the maximum force component was below 0.0001 au.

Acknowledgements

Thanks are due to the University of Aveiro and also to FCT and FEDER for funding the QOPNA Research Unit (project PEst-C/UI01/00062/2011) and the Portuguese National NMR Network. J.C.J.M.D.S.M. thanks QOPNA for a research grant. A.M.V.M.P. and S.M.S. acknowledge FCT for post-doc fellowships (SFRH/BPD/64693/2009 and SFRH/BPD/64752/2009). CAPES, CNPq and FAPERJ are also acknowledged for financial support (S.T.M., B.V.S. and A.C.P.).

Supplementary data

¹H, ¹³C, DEPT-135, COSY, NOESY, HSQC and HMBC NMR spectra, ESI HRMS, and UV–vis absorption spectra of the 1,3,3-trimethylindolin-2-ones **8a–c** and the porphyrin indolin-2-one conjugates **9a–g**. Supplementary data related to this article can be found online at <http://dx.doi.org/10.1016/j.tet.2012.07.024>.

References and notes

- Handbook of Porphyrin Science*; Kadish, K., Smith, K. M., Guillard, R., Eds.; World Scientific Publishing Company: Singapore, 2010; Vol. 4 & 12.
- See, for example: (a) Jaquinod, L. In *The Porphyrin Handbook*; Kadish, K., Smith, K. M., Guillard, R., Eds.; Academic: San Diego, 2000; Vol. 1; Chapter 5, pp 201–237; (b) Cavaleiro, J. A. S.; Tomé, A. C.; Neves, M. G. P. M. S. In *Handbook of Porphyrin Science*; Kadish, K., Smith, K. M., Guillard, R., Eds.; World Scientific Publishing Company: Singapore, 2010; Vol. 2; Chapter 9, pp 193–294; (c) Sergeeva, N. N.; Senge, M. O.; Ryan, A. In *Handbook of Porphyrin Science*; Kadish, K., Smith, K. M., Guillard, R., Eds.; World Scientific Publishing Company: Singapore, 2010; Vol. 3; Chapter 12, pp 325–365.
- (a) Fields, K. B.; Ruppel, J. V.; Snyder, N. L.; Zhang, X. P. In *Handbook of Porphyrin Science*; Kadish, K., Smith, K. M., Guillard, R., Eds.; World Scientific Publishing Company: Singapore, 2010; Vol. 3; Chapter 13, pp 367–427; (b) Takamami, T.; Hayashi, M.; Hino, F.; Suda, K. *Tetrahedron Lett.* **2003**, *44*, 7353; (c) Chen, Y.; Zhang, X. P. *J. Org. Chem.* **2003**, *68*, 4432; (d) Gao, G.-Y.; Chen, Y.; Zhang, X. P. *J. Org. Chem.* **2003**, *68*, 6215; (e) Soares, A. R. M.; Martínez-Díaz, M. V.; Brückner, A.; Pereira, A. M. V. M.; Tomé, J. P. C.; Alonso, C. M. A.; Faustino, M. A. F.; Neves, M. G. P. M. S.; Tomé, A. C.; Silva, A. M. S.; Cavaleiro, J. A. S.; Torres, T.; Guldi, D. M. *Org. Lett.* **2007**, *9*, 1557; (f) Pereira, A. M. V. M.; Alonso, C. M. A.; Neves, M. G. P. M. S.; Tomé, A. C.; Silva, A. M. S.; Paz, F. A. A.; Cavaleiro, J. A. S. *J. Org. Chem.* **2008**, *73*, 7353; (g) Pereira, A. M. V. M.; Neves, M. G. P. M. S.; Cavaleiro, J. A. S.; Jeandon, C.; Gisselbrecht, J.-P.; Choua, S.; Ruppert, R. *Org. Lett.* **2011**, *13*, 4742.
- (a) Shellard, E. J. *Bull. Narc.* **1974**, *26*, 41; http://www.unodc.org/unodc/en/data-and-analysis/bulletin/bulletin_1974-01-01_2_page005.html; (b) Keplinger, K.; Laus, G.; Wurm, M.; Dierich, M. P.; Teppner, H. *J. Ethnopharmacol.* **1999**, *64*, 23; (c) Reinhard, K.-H. *J. Alternative Complement. Med.* **1999**, *5*, 143; (d) Peddibhotla, S. *Curr. Bioact. Compd.* **2009**, *5*, 20.
- (a) Da Silva, J. F. M.; Garden, S. J.; Pinto, A. C. *J. Braz. Chem. Soc.* **2001**, *12*, 273; (b) Vine, K. L.; Matesic, L.; Locke, J. M.; Ranson, M.; Skropeta, D. *Anticancer Agents Med. Chem.* **2009**, *9*, 397.
- Gerchiaro, G.; Ferreira, A. M. C. *J. Braz. Chem. Soc.* **2006**, *17*, 1473.
- Papaetis, G. S.; Syrigos, K. N. *Biodrugs* **2009**, *23*, 377.
- (a) Shangary, S.; Wang, S. *Annu. Rev. Pharmacol. Toxicol.* **2009**, *49*, 223; (b) Dickens, M. P.; Fitzgerald, R.; Fischer, P. M. *Semin. Cancer Biol.* **2010**, *20*, 10.
- (a) Silva, B. V.; Ribeiro, N. M.; Pinto, A. C.; Vargas, M. D.; Dias, L. C. *J. Braz. Chem. Soc.* **2008**, *19*, 1244; (b) Silva, B. V.; Ribeiro, N. M.; Vargas, M. D.; Lanznaster, M.; Carneiro, J. W. M.; Krogh, R.; Andricopulo, A. D.; Dias, L. C.; Pinto, A. C. *Dalton Trans.* **2010**, *39*, 7338.
- Spencer, J.; Mendham, A. P.; Kotha, A. K.; Richardson, S. C. W.; Hillard, E. A.; Jaouen, G.; Male, L.; Hursthouse, M. B. *Dalton Trans.* **2009**, 918.
- The starting porphyrin **6** was prepared according to known procedures: (a) Rocha Gonsalves, A. M. d'A.; Varejão, J. M. T. B.; Pereira, M. M. *J. Heterocycl. Chem.* **1991**, *28*, 635; (b) Buchler, J. W. In *Porphyrins and Metalloporphyrins*; Smith, K. M., Ed.; Elsevier: Amsterdam, 1975; Chapter 5, pp 157–231; (c) Giraudeau, A.; Callot, H. J.; Jordan, J.; Ezhar, I.; Gross, M. *J. Am. Chem. Soc.* **1979**, *101*, 3857; (d) Hombrecher, H. K.; Gherdan, V. M.; Ohm, S.; Cavaleiro, J. A. S.; Neves, M. G. P. M. S.; Condeso, M. F. *Tetrahedron* **1993**, *49*, 8569.
- Ölgen, S.; Götz, C.; Jose, J. *Biol. Pharm. Bull.* **2007**, *30*, 715.
- The reactions were performed using conditions described in the literature: Kao, H.-C.; Hsu, C.-J.; Hsu, C.-W.; Lin, C.-H.; Wang, W.-J. *Tetrahedron Lett.* **2010**, *51*, 3743.
- Bruneau, P. A. R.; Crawley, G. C.; Oldham, K. European Patent 0 462 831 A2, 19 June 1991.
- For examples of generation of molecular ion and/or pseudomolecular ion under ESI conditions: (a) Quirke, J. M. E. In *The Porphyrin Handbook*; Kadish, K., Smith, K. M., Guillard, R., Eds.; Academic: San Diego, 2000; Vol. 7; Chapter 54, pp 371–416; (b) Van Berkel, G. J.; McLuckey, S. A.; Glush, G. L. *Anal. Chem.* **1991**, *63*, 1098; (c) Carvalho, C. M. B.; Neves, M. G. P. M. S.; Tomé, A. C.; Paz, F. A. A.; Silva, A. M. S.; Cavaleiro, J. A. S. *Org. Lett.* **2011**, *13*, 130.
- Macgregor, S. A. *Chem. Soc. Rev.* **2007**, *36*, 67.
- Microwave induced palladium-catalyzed amination of aryl halides: (a) Sharifi, A.; Hosseinzadeh, R.; Mirzaei, M. *Monatsh. Chem.* **2002**, *133*, 329; (b) Maes, B. U. W.; Loones, K. T. J.; Hostyn, S.; Diels, G.; Rombouts, G. *Tetrahedron* **2004**, *60*, 11559.
- Kwong, F. Y.; Klapars, A.; Buchwald, S. L. *Org. Lett.* **2002**, *4*, 581.
- (a) Zawisza, A. M.; Muzart, J. *Tetrahedron Lett.* **2007**, *48*, 6738; (b) Moon, J.; Lee, S. *J. Organomet. Chem.* **2009**, *694*, 473; (c) Chen, J.; Zhang, Y.; Yang, L.; Zhang, X.; Liu, J.; Li, L.; Zhang, H. *Tetrahedron* **2007**, *63*, 4266.
- Frisch, M. J.; Trucks, G. W.; Schlegel, H. B.; Scuseria, G. E.; Robb, M. A.; Cheeseman, J. R.; Montgomery, J. A., Jr.; Vreven, T.; Kudin, K. N.; Burant, J. C.; Millam, J. M.; Iyengar, S. S.; Tomasi, J.; Barone, V.; Mennucci, B.; Cossi, M.; Scalmani, G.; Rega, N.; Petersson, G. A.; Nakatsuji, H.; Hada, M.; Ehara, M.; Toyota, K.; Fukuda, R.; Hasegawa, J.; Ishida, M.; Nakajima, T.; Honda, Y.; Kitao, O.; Nakai, H.; Klene, M.; Li, X.; Knox, J. E.; Hratchian, H. P.; Cross, J. B.; Bakken, V.; Adamo, C.; Jaramillo, J.; Gomperts, R.; Stratmann, R. E.; Yazyev, O.; Austin, A. J.; Cammi, R.; Pomelli, C.; Ochterski, J. W.; Ayala, P. Y.; Morokuma, K.; Voth, G. A.; Salvador, P.; Dannenberg, J. J.; Zakrzewski, V. G.; Dapprich, S.; Daniels, A. D.; Strain, M. C.; Farkas, O.; Malick, D. K.; Rabuck, A. D.; Raghavachari, K.; Foresman, J. B.; Ortiz, J. V.; Cui, Q.; Baboul, A. G.; Clifford, S.; Cioslowski, J.; Stefanov, B. B.; Liu, G.; Liashenko, A.; Piskorz, P.; Komaromi, I.; Martin, R. L.; Fox, D. J.; Keith, T.; Al-Laham, M. A.; Peng, C. Y.; Nanayakkara, A.; Challacombe, M.; Gill, P. M. W.; Johnson, B.; Chen, W.; Wong, M. W.; Gonzalez, C.; Pople, J. A. *Gaussian 03, Revision D.02*; Gaussian: Wallingford CT, 2004.
- Elstner, M.; Porezag, D.; Jungnickel, G.; Elsner, J.; Haugk, M.; Frauenheim, T.; Suhai, S.; Seifert, G. *Phys. Rev. B* **1998**, *58*, 7260.
- Zheng, G.; Witek, H. A.; Bobadova-Parvanova, P.; Irlé, S.; Musaev, D. G.; Prabhakar, R.; Morokuma, K.; Lundberg, M.; Elstner, M.; Köhler, C.; Frauenheim, T. *J. Chem. Theory Comput.* **2007**, *3*, 1349.